# Guanidinium Para-Substituted Benzenesulfonates: Competitive Hydrogen Bonding in Layered Structures and the Design of Nonlinear Optical Materials

Victoria A. Russell,† Margaret C. Etter,†,§ and Michael D. Ward*,‡

*Department of Chemistry, University of Minnesota, Smith Hall, 207 Pleasant St. SE, Minneapolis, Minnesota 55455, and Department of Chemical Engineering and Materials Science, University of Minnesota, Amundson Hall, 421 Washington Ave. SE, Minneapolis, Minnesota 55455*

*Received February 2, 1994. Revised Manuscript Received March 17, 1994®*

X-ray crystal structures of six guanidinium para-substituted benzenesulfonates, $[C(NH_2)_3]^+(p\text{-}XC_6H_4SO_3]^-$ (X = $-CH_3$, $-NH_2$, $-OCH_3$, $-NO_2$, $-OH$, and $-CO_2H$), are reported. Molecular packing in these salts is directed predominantly by hydrogen-bonding and Coulombic interactions. The planar guanidinium–sulfonate hydrogen-bonded sheet motif that is generally observed for these compounds is disrupted when the substituent X has hydrogen-bonding character. Consequently, the sheets "pucker" about guanidinium–sulfonate hydrogen-bonded ribbons, the puckering increasing with increasing hydrogen-bonding ability of X. For X = $-CH_3$, $-NH_2$, and $-OCH_3$ the typical nearly planar sheet motif is observed. For X = $-NO_2$ and $-OH$, the puckering of the hydrogen-bonded sheets is severe, and the ribbons assemble into noncentrosymmetric crystalline phases (*Ama*2 and *Ima*2, respectively) which exhibit second harmonic generation. For X = $-CO_2H$, the sheet motif is completely disrupted due to competitive hydrogen bonding of X for guanidinium and sulfonate hydrogen-bonding sites. However, guanidinium–sulfonate hydrogen-bonded ribbons are observed in all salts. These studies suggest that the highly directing hydrogen-bonding and ionic character of the guanidinium–sulfonate networks provide a sound strategy for materials design, particularly for low-dimensional electronic properties and second harmonic generation.

## Introduction

Organic molecular materials often possess interesting electronic properties, including nonlinear optical behavior, electrical conductivity, superconductivity, and ferromagnetism.[1] Rational control over and predictability of molecular self-assembly processes are critical for intelligent crystal engineering, but control of molecular orientation in supramolecular structure is difficult and is recognized as a major obstacle in materials design.[2] Many attempts to control the structure of solids have focused on crystal engineering via charge-transfer,[3] electrostatic,[4] and hydrogen-bonding interactions. Use of hydrogen bonding to direct rationally the self-assembly of molecules into preordained packing motifs has been especially noteworthy in several classes of compounds,[5] including carboxylic acids,[6] nitroanilines,[7] imides,[8] and diarylureas.[9] These examples illustrate the considerable design flexibility provided by hydrogen bonding and have substantiated hydrogen-bonding "rules"[10] that can be used as guidelines for predicting packing motifs in hydrogen-bonded molecular crystals.

An intriguing area of materials engineering involves the design of noncentrosymmetric crystals for second harmonic generation (SHG). Several strategies have been employed

† Department of Chemistry, University of Minnesota.
‡ Department of Chemical Engineering and Materials Science, University of Minnesota.
§ Deceased June 10, 1992.
* To whom correspondence should be addressed.
® Abstract published in *Advance ACS Abstracts,* August 15, 1994.

(1) (a) *Nonlinear Optical Properties of Organic Molecules and Crystals*; Chemla, D. S., Zyss, J., Eds.; Academic Press: Orlando, FL, 1987; Vol. 1. (b) *Extended Linear Chain Compounds*; Miller, J. S., Ed.; Plenum: New York, 1982–1983; Vols. 1–3.

(2) Desiraju, G. R. *Crystal Engineering: The Design of Organic Solids*; Elsevier: New York, 1989.

(3) Herbstein, F. H. In *Perspective in Structural Chemistry*, Dunitz, J. D., Ibers, J. A., Eds.; Wiley and Sons: New York, 1971; Vol. 4, pp 166–395.

(4) (a) Ward, M. D.; Fagan, P. J.; Calabrese, J. C.; Johnson, D. C. *J. Am. Chem. Soc.* **1989**, *111*, 1719. (b) Fagan, P. J.; Ward, M. D.; Calabrese, J. C. *J. Am. Chem. Soc.* **1989**, *111*, 1698.

(5) For recent work on use of hydrogen bonding for designed structures see: (a) Lehn, J.-M.; Mascal, M.; DeCian, A.; Fischer, J. *J. Chem. Soc., Perkin Trans. 2* **1992**, 461. (b) Lehn, J.-M.; Mascal, M.; DeCian, A.; Fischer, J. *J. Chem. Soc., Chem. Commun.* **1990**, 479. (c) Fouquey, C.; Lehn, J.-M.; Levelut, A.-M. *Adv. Mater.* **1990**, *2*, 254. (d) Zerowski, J. A.; Seto, C. T.; Whitesides, G. M. *J. Am. Chem. Soc.* **1992**, *114*, 5473. (e) Seto, C. T.; Whitesides, G. M. *J. Am. Chem. Soc.* **1991**, *113*, 712. (f) Whitesides, G. M.; Mathias, J. P.; Seto, C. T. *Science* **1991**, *254*, 1312. (g) Zerowski, J. A.; Seto, C. T.; Wierda, D. A.; Whitesides, G. M. *J. Am. Chem. Soc.* **1990**, *112*, 9025. (h) Seto, C. T.; Whitesides, G. M. *J. Am. Chem. Soc.* **1990**, *112*, 6409. (i) Persico, F.; Wuest, J. D. *J. Org. Chem.* **1993**, *58*, 95. (j) Simard, M.; Su, D.; Wuest, J. D. *J. Am. Chem. Soc.* **1991**, *113*, 4696. (k) Ducharme, Y.; Wuest, J. D. *J. Org. Chem.* **1988**, *53*, 5787. (l) Gallant, M.; Biet, M. T. P.; Wuest, J. D. *J. Org. Chem.* **1991**, *56*, 2284. (m) Scoponi, M.; Polo, E.; Pradella, F.; Bertolasi, V.; Carassiti, V.; Goberti, P. *J. Chem. Soc., Perkin Trans. 2* **1992**, 1127. (n) Chang, Y.-L.; West, M.-A.; Fowler, F. W.; Lauher, J. W. *J. Am. Chem. Soc.* **1993**, *115*, 5991. (o) Lauher, J. W.; Chang, Y.-L.; Fowler, F. W. *Mol. Cryst. Liq. Cryst.* **1992**, *211*, 99. (p) Zhao, X.; Chang, Y.-L.; Fowler, F. W.; Lauher, J. W. *J. Am. Chem. Soc.* **1990**, *112*, 6627. (q) Hollingsworth, M. D.; Santansiero, B. D.; Oumar-Mahamat, H.; Nichols, C. J. *Chem. Mater.* **1991**, *3*, 23. (r) Garcia-Tellado, F.; Geib, S. J.; Goswami, S.; Hamilton, A. D. *J. Am. Chem. Soc.* **1991**, *113*, 9265.

(6) Frankenbach, G. M.; Etter, M. C. *Chem. Mater.* **1992**, *4*, 272.

(7) (a) Etter, M. C.; Huang, K. S. *Chem. Mater.* **1992**, *4*, 824. (b) Etter, M. C.; Huang, K. S.; Frankenbach, G. M.; Adsmond, D. A. In *Materials for Nonlinear Optics, Chemical Perspectives*; Marder, S. R., Sohn, J. E., Stucky, G. D., Eds.; ACS Symposium Series 455; American Chemical Society: Washington, DC, 1991; pp 446–455. (c) Panunto, T. W.; Urbánczyk-Lipkowska, Z.; Johnson, R.; Etter, M. C. *J. Am. Chem. Soc.* **1987**, *109*, 7786.

(8) (a) Reutzel, S. M.; Etter, M. C. *J. Phys. Org. Chem.* **1992**, *5*, 44. (b) Etter, M. C.; Reutzel, S. M. *J. Am. Chem. Soc.* **1991**, *113*, 2586.

(9) Etter, M. C.; Urbánczyk-Lipkowska, Z.; Zia-Ebrahimi, M.; Panunto, T. W. *J. Am. Chem. Soc.* **1990**, *112*, 8415.

0897-4756/94/2806-1206$04.50/0 

**Chart 1**

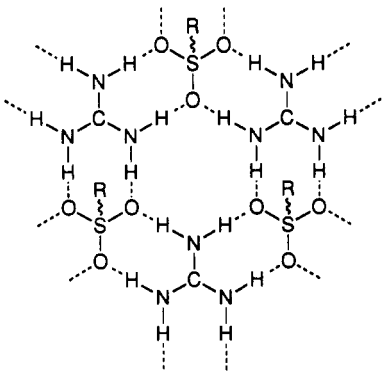

R = alkyl- or aryl-

for this purpose, including use of chiral molecules to force crystallization into noncentrosymmetric space groups, synthesis of acentric host–guest complexes, electric field poling of polymers, and acentric orientation of Langmuir–Blodgett films. Crystal engineering approaches using hydrogen-bonding interactions to direct crystallization into noncentrosymmetric structures have also been attempted.[6,7a,c,10a,11] However, centrosymmetric space groups generally are highly preferred because of more favorable intermolecular dipole–dipole interactions and greater facility of close-packing. As shown from database studies of nitroanilines[7a] and benzoic acids[6] as well as from cocrystallization studies,[7c,9,11a] hydrogen-bonding interactions can be used to overcome dipole–dipole interactions, increasing the chance of forming noncentrosymmetric lattices. Recently, organic salts with large second-order optical nonlinearities have been reported,[12] suggesting that Coulombic interactions in salts may override and screen the dipolar interactions which favor centrosymmetric arrangements. SHG also has been reported in hydrogen-bonded salts of organic cations with inorganic anions.[13] These reports strongly suggest that crystal engineering strategies which employ ionic hydrogen bonding networks represent an intelligent approach to the design of acentric materials.

We previously reported that guanidinium sulfonates, $[C(NH_2)_3]^+[RSO_3]^-$ formed unique two-dimensional hydrogen-bonded networks (Chart 1) in the solid state[14] if R was a simple alkane or arene moiety.[15] The hydrogen-bonded network was maintained in all cases, although the size of the R group affected the assembly of the hydrogen-bonded layers in the third dimension. These studies demonstrated that proper combination of molecular topology and hydrogen bonding can lead to substantial control over crystal packing. The synthesis of related compounds with desirable electronic properties will require functionalized R groups with appropriate electronic structure or polarizability, demanding examination of the influence of R-group substituents on the hydrogen-bonding motif. Specifically, hydrogen-bonding substituents on the alkane- or arenesulfonate may compete for hydrogen-bonding sites in the guanidinium sulfonate network, thereby influencing the sheet motif. Herein we report the X-ray crystal structures of six guanidinium para-substituted benzenesulfonates, $[C(NH_2)_3]^+[p\text{-}XC_6H_4SO_3]^-$, where the X substituent varies in hydrogen-bonding ability: X = $-CH_3$, $-NH_2$, $-OCH_3$, $-NO_2$, $-OH$, and $-CO_2H$. We examine the effect of the substituent X, specifically its hydrogen-bonding ability, on the structure of the hydrogen-bonded sheets and the three-dimensional packing of these sheets. These results demonstrate that hydrogen-bonding substituents on the arenesulfonate component are capable of disrupting the planarity of the guanidinium–sulfonate network, resulting in a "puckering" of the sheets which increases with increasing hydrogen-bonding ability. The crystal structures also suggest that noncentrosymmetric phases are possible when this puckering is severe. The polar axes in these cases are described by the dipole orientation of the R groups situated on opposite sides of the puckered sheets. These observations suggest that the combination of hydrogen bonding and ionic networks favors the formation of the noncentrosymmetric phases.

## Experimental Section

**Materials.** All commercially available starting materials were purchased from the companies indicated and used as received. *p*-Anisolesulfonic acid was synthesized by conventional methods.[16] Spectroscopic-grade solvents and/or deionized water were used for all crystallizations.

**Characterization.** Melting points were determined by differential scanning calorimetry (DSC) on a Mettler FP80/FP84 (100 mV, 1 °C/min) or with a Fisher-Johns hot stage apparatus (F-J) and are uncorrected. Solid-state infrared spectra were recorded on a Nicolet 510M spectrometer (4-$cm^{-1}$ resolution) as Nujol mulls. $^1H$ NMR spectra were recorded on an IBM NR200AF spectrometer (200 MHz) in $(CD_3)_2SO$ (Cambridge Isotope Laboratories) relative to internal standard TMS. Elemental analysis was obtained from M-H-W Laboratories, Phoenix, AZ. SHG activity was measured on a modified Kurtz and Perry[17]-design single-beam powder analyzer and referenced to urea. Samples used were unsized microcrystalline powders obtained by grinding and prepared as fluorolube mulls placed on microscope slides with cover slips. A Nd:YAG laser (Kigre, MK-20) emitting at 1064 nm with 20 mJ/pulse was used, and the frequency-doubled green beam at 532 nm was observed through bandpass filters. A Hewlett-Packard 54200A oscilloscope was used to monitor the signal.

(10) (a) Etter, M. C. *J. Phys. Chem.* **1991**, *95*, 4601. (b) Etter, M. C. *Acc. Chem. Res.* **1990**, *23*, 120.

(11) (a) Etter, M. C.; Frankenbach, G. M.; Adsmond, D. A. *Mol. Cryst. Liq. Cryst.* **1990**, *187*, 25. (b) Etter, M. C.; Frankenbach, G. M. *Chem. Mater.* **1989**, *1*, 10. (c) Etter, M. C. *Isr. J. Chem.* **1985**, *25*, 312. (d) Etter, M. C. *J. Am. Chem. Soc.* **1982**, *104*, 1095.

(12) (a) Marder, S. R.; Perry, J. W.; Schaefer, W. P. *J. Mater. Chem.* **1992**, *2*, 985. (b) Marder, S. R.; Perry, J. W.; Schaefer, W. P. *Science* **1989**, *245*, 626.

(13) (a) Aakeroy, C. B.; Hitchcock, P. B.; Moyle, B. D.; Seddon, K. R. *J. Chem. Soc., Chem. Commun.* **1989**, 1856. (b) Aakeroy, C. B.; Azoz, N.; Calvert, P. D.; Kadim, M.; McCaffery, A. J.; Seddon, K. R. In *Materials for Nonlinear Optics: Chemical Perspectives*; Marder, S. R., Sohn, J. E., Stucky, G. D., Eds.; American Chemical Society: Washington, DC, 1991; Chapter 34, pp 516–527. (c) Aakeroy, C. B.; Hitchcock, P. B.; Seddon, K. R. *J. Chem. Soc., Chem. Commun.* **1992**, 553.

(14) Russell, V. A.; Etter, M. C.; Ward, M. D. *J. Am. Chem. Soc.*, **1994**, *116*, 1941.

(15) The formation of guanidinium alkane- and arenesulfonate salts was also reported previously, although no spectroscopic or structural data were given. (a) Karrer, P.; Epprecht, A. *Helv. Chim. Acta* **1941**, *24*, 310. (b) Short, W. F.; Oxley, P. British Patent 593,695; *Chem. Abstr.* **1948**, *42*, 1965i.

(16) *p*-Anisolesulfonic acid was synthesized as follows: Anisole (10.00 g, 0.092 mol) and concentrated sulfuric acid (9.45 g, 0.092 mol) were heated at 65–75 °C for 30 min with stirring. The solution solidified to a hardened white mass. Over time, the solid dissolved and light tan plates of *p*-anisolesulfonic acid crystallized slowly. Yield: 9.31 g, 0.050 mol, 54%. Note that the reaction is quantitative, but the yield reported here is of crystals obtained after a very slow crystallization, rather than the crude powder; mp 76–82 °C (Fisher-Johns melting point apparatus). IR 2211 (br), 1906 (br), 1738, 1713, 1596, 1576, 1499, 1465, 1412, 1378, 1310, 1262, 1189, 1127, 1113, 1098, 1025, 1000, 835, 818, 805, 724, 677, 629 $cm^{-1}$; $^1H$ NMR $\delta$ 7.53 (d, 2 H, $J$ = 8.7 Hz, Ar-*H* ortho to $SO_3$), 6.87 (d, 2 H, $J$ = 8.7 Hz, Ar-*H* meta to $SO_3$), 3.76 (s, 3 H, Ar-$OCH_3$); Elemental analysis indicated that the product may be hydrated: Calcd unhydrated/monohydrate (found) for $C_7H_8O_3S$: C 44.67/40.77 (39.25), H 4.28/4.89 (5.36), S 17.04/15.55 (15.75). The experimentally determined elemental analysis suggest that this compound is multiply hydrated and/or slightly impure.

(17) Kurtz, S. K.; Perry, T. T. *J. Appl. Phys.* **1968**, *39*, 3798.

**Table 1. Crystallographic Data for Guanidinium Sulfonates 1–6**

| | 1 | 2 | 3 | 4 | 5 | 6 |
|---|---|---|---|---|---|---|
| | | | (A) Crystal Parameters | | | |
| formula | $C_8H_{13}N_3O_3S$ | $C_7H_{12}N_3O_3S$ | $C_8H_{13}N_3O_4S$ | $C_7H_{10}N_4O_5S$ | $C_7H_{11}N_3O_4S$ | $C_8H_{11}N_3O_5S$ |
| FW | 231.27 | 232.26 | 247.27 | 262.24 | 233.24 | 261.25 |
| crystal size ($mm^3$) | 0.55 × 0.50 × 0.45 | 0.60 × 0.20 × 0.08 | 0.55 × 0.45 × 0.20 | 0.60 × 0.34 × 0.25 | 0.60 × 0.25 × 0.25 | 0.45 × 0.40 × 0.25 |
| space group | monoclinic | monoclinic | monoclinic | orthorhombic | orthorhombic | monoclinic |
| crystal system | $P2_1/c$ | $P2_1/c$ | $P2_1/c$ | $Ama2$ | $Ima2$ | $P2_1/a$ |
| $a$ (Å) | 12.437 (3) | 12.182 (3) | 12.119 (8) | 7.471 (8) | 7.191 (4) | 7.191 (3) |
| $b$ (Å) | 7.418 (4) | 7.453 (4) | 7.432 (2) | 20.690 (7) | 17.345 (5) | 15.602 (3) |
| $c$ (Å) | 25.72 (3) | 25.046 (8) | 27.587 (6) | 7.340 (2) | 7.899 (3) | 10.614 (2) |
| $\beta$ (deg) | 95.56 (6) | 97.26 (2) | 94.53 (3) | 90 | 90 | 103.33 (3) |
| $V$ (Å$^3$) | 2362 (4) | 2256 (2) | 2477 (3) | 1135 (2) | 985 (1) | 1159 (1) |
| $Z$ | 8 | 8 | 8 | 4 | 4 | 4 |
| $d_{calc}$(g/cm$^3$) | 1.301 | 1.368 | 1.326 | 1.535 | 1.572 | 1.497 |
| $F(000)$ | 976 | 976 | 1040 | 544 | 488 | 544 |
| $\mu$(Mo K$\alpha$)(cm$^{-1}$) | 2.55 | 2.69 | 2.53 | 2.89 | 3.13 | 2.80 |
| | | | (B) Data Collection | | | |
| $2\theta_{max}$ (deg) | 48.0 | 47.9 | 50.0 | 55.9 | 55.9 | 55.9 |
| data collected ($hkl$) | ±14, +8, ±29 | +13, ±8, ±28 | +13, ±8, ±31 | ±9, +9, +27 | ±9, +10, +22 | ±9, +20, ±14 |
| scan speed (deg/min in $\omega$) | 8.3–16.5 | 16.5 | 1.0–8.3 | 8.2 | 16.5 | 16.5 |
| reflections collected | 6241 | 4109 | 5620 | 3006 | 1312 | 5162 |
| unique reflections | 4034 | 3850 | 4721 | 1617 | 708 | 2905 |
| $R$(merg) (%) | 3.4 | 3.3 | 6.6 | 3.9 | 2.6 | 3.3 |
| corrections applied[a] | 1, 2 | 1, 2 | 2 | | 1 | 1 |
| | | | (C) Refinement | | | |
| $R(F)$[b] (%) | 5.2 | 6.0 | 6.1 | 4.8 | 3.5 | 4.4 |
| $R(wF)$[c] (%) | 6.1 | 5.5 | 6.1 | 4.7 | 4.7 | 5.3 |
| $\Delta/\sigma$(max) | 0.08 | 0.00 | 0.00 | 0.00 | 0.00 | 0.01 |
| $\Delta(\rho)$ (e$^-$/Å$^3$) | 0.24 | 0.28 | 0.30 | 0.21 | 0.31 | 0.20 |
| indep refl obs $F_o > 2\sigma(F_o)$ | 2469 | 1982 | 2181 | 1165 | 635 | 1884 |
| $N_o/N_v$ | 9.08 | 7.29 | 7.52 | 10.89 | 7.56 | 11.92 |
| GOF | 1.43 | 1.38 | 1.72 | 1.62 | 1.38 | 1.25 |

[a] All structures were corrected for Lorentz and polarization effects. 1 = empirical absorption using DIFABS (Walker, N.; Stuart, D. *Acta Crystallogr.* **1983**, *A39*, 158–166); 2 = secondary extinction. [b] $R(F) = \sum||F_o| - |F_c||/|F_o|$. [c] $R(wF) = [(\sum w(|F_o| - |F_c|)^2/\sum wF_o^2)]^{1/2}$; $w = 4F_o^2/\sigma^2(F_o)^2$.

Experimental details of the X-ray analyses of the salts presented here are given in Table 1. Single-crystal X-ray structural data were collected on an Enraf-Nonius CAD4 diffractometer with graphite-monochromated Mo K$\alpha$ radiation ($\lambda$ = 0.710 69) using the $\omega$-scan technique at 24 °C. Lattice parameters were obtained from least-squares analysis of 22–25 reflections (except **2**, in which 49 reflections were used). Three standard reflections were measured every 50–70 min. All structures were corrected for Lorentz and polarization effects, other corrections are noted in Table 1. Structures were solved by direct methods with MITHRIL[18] and DIRDIF.[19] All non-hydrogen atoms were refined anisotropically. Hydrogen atoms included in the structure factor calculations were placed in idealized positions ($d_{C-H}$ = 0.95 Å, and $d_{N-H}$ = 0.95 for **1–3**, **5**, and **6**) with assigned isotropic thermal parameters ($B$ = 1.2$B$ of bonded atoms) except for **4**, whose guanidinium N–H protons (distances N1–H1 0.86 (3), N2–H3 0.86 (3), N2–H4 0.92 (5) Å) were refined with isotropic temperature factors (H1 4.2 (2), H3 4.4 (7), H4 4.8 (8)). In **1** the methyl hydrogens are probably disordered and are put in at positions that best agree with the Fourier difference map. In **5** the hydroxyl proton was not located in the structure determination.

**Synthesis of Guanidinium Sulfonates.** Guanidinium sulfonates were prepared by slow evaporation of solutions of guanidine hydrochloride (Aldrich Chemical Co.) or guanidine carbonate (Sigma Chemical Co.) and the appropriate sulfonic acid or potassium sulfonate under ambient conditions. Crystals were removed from solution prior to complete evaporation of the solvent.

**Guanidinium Tosylate (Guanidinium *p*-Toluenesulfonate) (1).** Crystallized from methanol solution containing equimolar quantities of guanidine hydrochloride and *p*-toluenesulfonic acid monohydrate (Aldrich) as colorless hexagonal prisms or from water as hexagonal and trigonal plates; mp 232–233 °C (DSC); IR 3358, 3336, 3260, 3194, 1678, 1579, 1459, 1377, 1188, 1126, 1037, 1012, 815, 687 cm$^{-1}$; $^1$H NMR $\delta$ 7.49 (d, 2 H, $J$ = 8.1 Hz, Ar-*H* ortho to $SO_3$), 7.14 (d, 2 H, $J$ = 7.9 Hz, Ar-*H* meta to $SO_3$), 6.96 (s, 6 H, $[C(NH_2)_3]^+$), 2.31 (s, 3 H, Ar–$CH_3$). Anal. Calcd (found) for $C_8H_{13}N_3O_3S$: C 41.55 (41.73), H 5.67 (5.55), N 18.17 (18.11), S 13.87 (13.96); SHG 0.

**Guanidinium Sulfanilate (Guanidinium *p*-Aminobenzenesulfonate) (2).** Crystallized from aqueous solution containing 1 equiv of guanidine carbonate and 2 equiv of sulfanilic acid (Aldrich) as colorless or tannish platelike needles; endotherms 175–180 (not observed for powdered sample), 221–222 (mp) °C (DSC); IR 3467, 3375, 3332, 3259, 3186, 2221, 1903, 1679, 1634, 1620, 1603, 1588, 1576, 1503, 1463, 1378, 1299, 1191, 1163, 1127, 1034, 1003, 830, 814, 743, 702 cm$^{-1}$; $^1$H NMR $\delta$ 7.26 (d, 2 H, $J$ = 8.5 Hz, Ar-*H* ortho to $SO_3$), 7.01 (s, 6 H, $[C(NH_2)_3]^+$), 6.46 (d, 2 H, $J$ = 8.5 Hz, Ar-*H* meta to $SO_3$), 5.24 (s, 2 H, Ar-$NH_2$). Anal. Calcd (found) for $C_7H_{12}N_4O_3S$: C 36.20 (36.44), H 5.21 (5.37), N 24.12 (24.27), S 13.81 (13.61); SHG 0.

**Guanidinium *p*-Anisolesulfonate (Guanidinium *p*-Methoxybenzenesulfonate) (3).** Crystallized from methanol solution containing 1 equivalent of guanidine carbonate and 2 equiv of *p*-anisolesulfonic acid as colorless rods from water or as colorless needles from methanol or 4:1 acetonitrile–water; endotherms 136–140, 207, 212–215 °C (DSC), mp 227–240 °C (F-J); IR 3370 (sh), 3338, 3261, 3193, 1681, 1605, 1580, 1501, 1463, 1378, 1308, 1266, 1185, 1129, 1036, 1003, 832, 803, 720, 689 cm$^{-1}$; $^1$H NMR $\delta$ 7.53 (d, 2 H, $J$ = 8.5 Hz, Ar-*H* ortho to $SO_3$), 6.97 (s, 6 H, $[C(NH_2)_3]^+$), 6.87 (d, 2 H, $J$ = 8.6 Hz, Ar-*H* meta to $SO_3$), 3.76 (s, 3 H, Ar-$OCH_3$). Anal. Calcd (found) for $C_8H_{13}N_3O_4S$: C 38.85 (38.61), H 5.30 (5.40), N 16.99 (16.78), S 12.97 (13.12); SHG 0. Note that *p-anisolesulfonic acid* must be used as a starting reagent rather than its sodium salt, otherwise sodium ion is incorporated into the crystal resulting in guanidinium sodium bis(*p*-anisolesulfonate) monohydrate.[20]

**Guanidinium *p*-Nitrobenzenesulfonate (4).** Crystallized from methanol solution containing equimolar quantities of guanidine hydrochloride and *p*-nitrobenzenesulfonic acid (Kodak)

(18) Gilmore, C. J. *J. Appl. Cryst.* **1984**, *17*, 42.

(19) Beurskens, P. T.; Bosman, W. P.; Doesburg, H. M.; Gould, R. O.; Van den Hark, Th. E. M.; Prick, P. A. J.; Noordik, J. H.; Beurskens, G.; Parthasarathi, V.; Bruins Slot, H. J.; Haltiwanger, R. C. DIRDIF: Direct Methods for Difference Structures; Technical Report 1984/1; Crystallography Laboratory, Toernooiveld, 6525 Ed Nijmegen, The Netherlands, 1984.

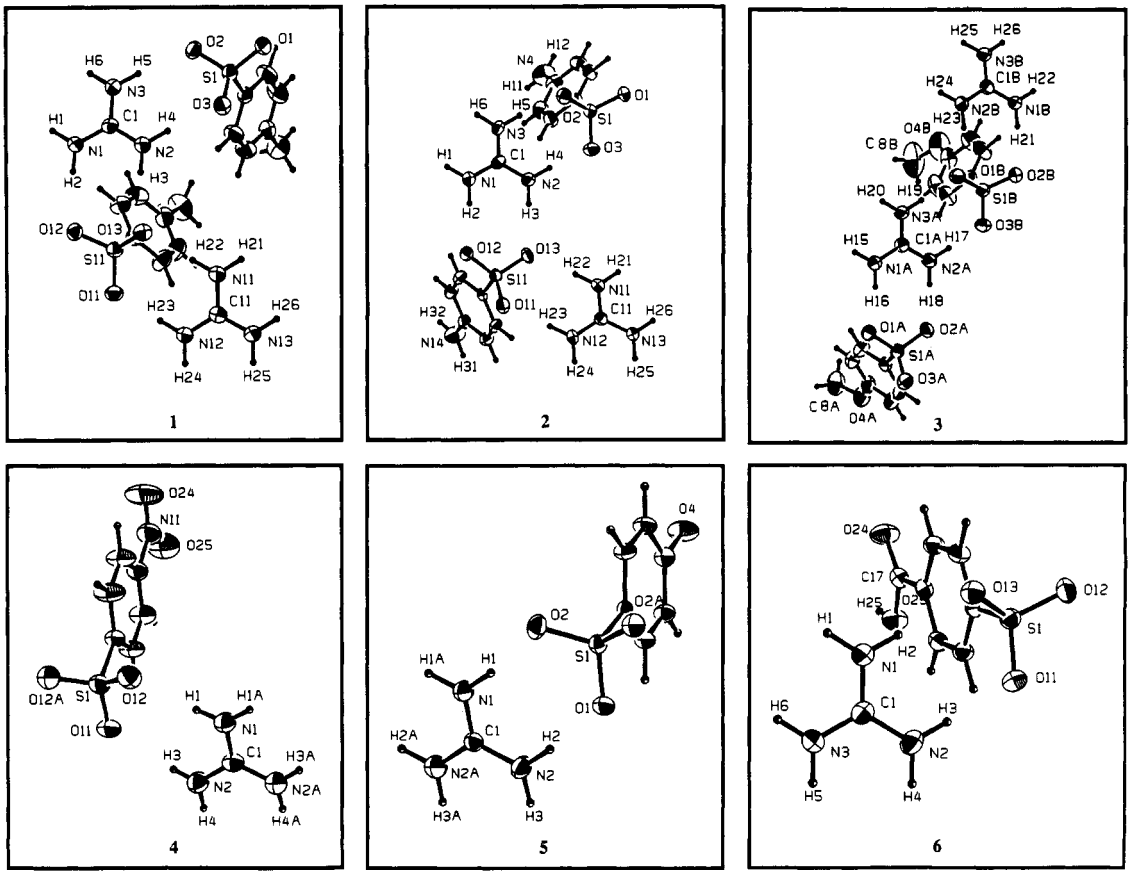


**Figure 1.** ORTEP drawings (30% probability ellipsoids) of asymmetric units and atom numbering schemes of **1–6**. Guanidinium–sulfonate hydrogen-bonded ribbon direction is approximately horizontal in each drawing. Note that in **5**, the hydroxyl proton was not located in the structure determination.

as light tan rectangular needles; mp 258–259 °C (DSC); IR 3406, 3367, 3211, 1669, 1607, 1573, 1528, 1460, 1377, 1349, 1196, 1127, 1036, 1011, 857, 749, 652 cm$^{-1}$; $^1$H NMR $\delta$ 8.23 (d, 2 H, $J$ = 8.8 Hz, Ar-*H* ortho to $SO_3$), 7.85 (d, 2 H, $J$ = 8.8 Hz, Ar-*H* meta to $SO_3$), 6.94 (s, 6 H, $[C(NH_2)_3]^+$). Anal. Calcd (found) for $C_7H_{10}N_4O_5S$: C 32.06 (32.18), H 3.84 (4.01), N 21.36 (21.39), S 12.23 (12.31); SHG 0.75 × urea.

**Guanidinium *p*-Hydroxybenzenesulfonate (5).** Crystallized from methanol solution containing equimolar quantities of guanidine hydrochloride and *p*-hydroxybenzenesulfonic acid (65 w/w aqueous solution) as colorless to light pinkish-tan needles; mp 189–192 °C (F-J), endotherm 180–190 (br, mp) °C (DSC); IR 3430, 3368, 3267, 3192, 1680, 1665, 1598, 1505, 1462, 1377, 1357, 1344, 1303, 1268, 1186, 1169, 1125, 1031, 1007, 838, 823, 809, 742 cm$^{-1}$; $^1$H NMR $\delta$ 9.57 (s, 1 H, Ar-O*H*), 7.42 (d, 2 H, $J$ = 8.5 Hz, Ar-*H* ortho to $SO_3$), 6.98 (s, 6 H, $[C(NH_2)_3]^+$), 6.68 (d, 2 H, $J$ = 8.5 Hz, Ar-*H* meta to $SO_3$). Anal. Calcd (found) for $C_7H_{11}N_3O_4S$: C 36.05 (35.97), H 4.75 (5.00), N 18.02 (17.81), S 13.75 (13.66); SHG 0.5 × urea.

**Guanidinium *p*-Carboxybenzenesulfonate (6).** Crystallized from 20% aqueous methanol solution containing equimolar quantities of guanidine hydrochloride and *p*-sulfobenzoic acid, monopotassium salt (Kodak) as thin colorless needles; mp 281 °C (DSC); IR 3474, 3428, 3349, 3260, 3194, 1684, 1647, 1574, 1462, 1377, 1252, 1231, 1183, 1166, 1183, 1112, 1030, 1004, 917, 804, 769, 712, 692 cm$^{-1}$; $^1$H NMR $\delta$ 13.00 (s, 1 H, Ar-COO*H*), 7.91 (d, 2 H, $J$ = 8.3 Hz, Ar-*H* ortho to $SO_3$), 7.70 (d, 2 H, $J$ = 8.4 Hz, Ar-*H* meta to $SO_3$), 6.93 (s, 6 H, $[C(NH_2)_3]^+$. Anal. Calcd (found) for $C_8H_{11}N_3O_5S$: C 36.78 (36.80), H 4.24 (4.23), N 16.08 (15.90), S 12.27 (12.16); SHG 0.

(20) Guanidinium sodium bis(*p*-anisolesulfonate) monohydrate: colorless needles; IR (Nujol) 3442, 3371, 3338, 3263, 3195, 1673, 1607, 1580, 1503, 1463, 1378, 1366 (sh), 1310, 1266, 1212, 1183, 1175, 1129, 1111, 1038, 1025, 1005, 832, 820, 805, 722, 685 cm$^{-1}$. X-ray structural data: $C_{15}H_{22}N_3O_9S_2Na$, FW 475.46, monoclinic, $P2_1/n$, $a$ = 10.693 (4), $b$ = 7.296 (3), $c$ = 27.008 (9) Å, $\beta$ = 96.46 (3)°, $V$ = 2094 (2) Å$^3$, $Z$ = 4, $d_{calc}$ = 1.508 g/cm$^3$, $F(000)$ = 992, $\lambda$(Mo K$\alpha$) = 0.710 69 Å, $\mu$(Mo K$\alpha$) = 3.13 cm$^{-1}$, $T$ = 297 K, $R(F)$ = 4.5%, $R(wF)$ = 5.4% for 2530 independent observed reflections ($N_o/N_v$ = 8.94).

## Results

**Molecular Structures.** X-ray quality crystals of guanidinium sulfonates can be grown by slow evaporation at ambient conditions of solutions containing guanidinium salts and the appropriate sulfonic acid. Guanidinium para-substituted benzenesulfonates crystallize in various monoclinic and orthorhombic space groups (Table 1). ORTEP views of the asymmetric units and atomic labeling are given in Figure 1. Selected intramolecular bond geometries (C–N, S–O, and relevant X group geometries) are given in Table 2. The respective structures of the guanidinium and sulfonate ions are similar for each salt, with delocalization evident in both guanidinium and sulfonate groups (average $d_{C-N}$ 1.321 ± 0.007 Å, $\theta_{N-C-N}$ 120.0 ± 0.5°, $d_{S-O}$ 1.457 ± 0.006 Å, $\theta_{O-S-O}$ 112.3 ± 0.7°). Other intramolecular bond lengths and angles for these salts are available as supplementary material (see paragraph at end of paper). The C–N lengths observed in our compounds agree with those found in a database study of unsubstituted guanidinium ion (mean $d_{C-N}$ 1.321 ± 0.008 Å)[21] and a theoretical calculation of guanidinium C–N lengths (1.321 and 1.334 Å).[22] The sulfonate S–O geometries compare well with those found in other sulfonate structures. In **4**, the nitro group and one sulfonate oxygen are coplanar with the aromatic ring. In **6**, the carboxyl group is approximately coplanar with the aromatic ring (3° out-of-plane). Table 2 lists other specific geometries of the para substituents.

(21) Allen, F. H.; Kennard, O.; Watson, D. G.; Brammer, L.; Orpen, A. G.; Taylor, R. *J. Chem. Soc., Perkin Trans. 2* **1987**, S1.
(22) Gobbi, A.; Frenking, G. *J. Am. Chem. Soc.* **1993**, *115*, 2362.

**Table 2. Selected Intramolecular Bond Lengths and Angles for 1–6**

| compound | $d_{C-N}$ (Å) | | $\theta_{N-C-N}$ (deg) | | $d_{S-O}$ (Å) | | $\theta_{O-S-O}$ (deg) | | Y–Z | $d_{Y-Z}$ (Å) | Z–Y–Z′ | $\theta_{Z-Y-Z'}$ (deg) |
|---|---|---|---|---|---|---|---|---|---|---|---|---|
| 1 | C1–N1 | 1.311 (5) | N1–C1–N2 | 120.3 (3) | S1–O1 | 1.453 (3) | O1–S1–O2 | 112.0 (2) | | | | |
| | C1–N2 | 1.327 (5) | N1–C1–N3 | 120.4 (4) | S1–O2 | 1.454 (3) | O1–S1–O3 | 113.0 (2) | | | | |
| | C1–N3 | 1.324 (5) | N2–C1–N3 | 119.3 (4) | S1–O3 | 1.451 (3) | O2–S1–O3 | 112.0 (2) | | | | |
| | C11–N11 | 1.321 (5) | N11–C11–N12 | 120.5 (4) | S11–O11 | 1.456 (3) | O11–S11–O12 | 113.2 (2) | | | | |
| | C11–N12 | 1.314 (5) | N11–C11–N13 | 119.7 (4) | S11–O12 | 1.454 (3) | O11–S11–O13 | 112.1 (2) | | | | |
| | C11–N13 | 1.335 (5) | N12–C11–N13 | 119.9 (3) | S11–O13 | 1.456 (3) | O12–S11–O13 | 111.9 (2) | | | | |
| 2 | C1–N1 | 1.323 (7) | N1–C1–N2 | 119.1 (5) | S1–O1 | 1.464 (4) | O1–S1–O2 | 111.3 (2) | N4–H11 | 0.949[a] | H11–N4–H12 | 120.21[a] |
| | C1–N2 | 1.328 (7) | N1–C1–N3 | 120.6 (6) | S1–O2 | 1.457 (4) | O1–S10–O3 | 112.9 (3) | N4–H12 | 0.949[a] | | |
| | C1–N3 | 1.303 (6) | N2–C1–N3 | 120.3 (6) | S1–O3 | 1.455 (4) | O2–S1–O3 | 112.1 (3) | | | | |
| | C11–N11 | 1.321 (6) | N11–C11–N12 | 120.1 (6) | S11–O11 | 1.456 (4) | O11–S11–O12 | 113.1 (2) | N14–H31 | 0.948[a] | H31–N14–H32 | 120.32[a] |
| | C11–N12 | 1.318 (7) | N11–C11–N13 | 119.7 (6) | N11–O12 | 1.462 (4) | O11–S11–O13 | 111.9 (2) | N14–H32 | 0.949[a] | | |
| | C11–N13 | 1.330 (7) | N12–C11–N13 | 120.1 (5) | S11–O13 | 1.468 (4) | O12–S11–O13 | 111.4 (2) | | | | |
| 3 | C1A–N1A | 1.322 (7) | N1A–C1A–N2A | 119.1 (5) | S1A–O1A | 1.468 (4) | O1A–S1A–O2A | 112.2 (2) | O4A–C8A($H_3$) | 1.424 (8) | | |
| | C1A–N2A | 1.333 (8) | N1A–C1A–N3A | 120.9 (5) | S1A–O2A | 1.460 (4) | O1A–S1A–O3A | 112.6 (3) | | | | |
| | C1A–N3A | 1.313 (6) | N2A–C1A–N3A | 120.0 (6) | S1A–O3A | 1.453 (4) | O2A–S1A–O3A | 112.0 (3) | | | | |
| | C1B–N1B | 1.312 (7) | N1B–C1B–N2B | 119.5 (5) | S1B–O1B | 1.462 (4) | O11–S1B–O2B | 111.9 (2) | O4B–C8B($H_3$) | 1.40 (1) | | |
| | C1B–N2B | 1.328 (7) | N1B–C1B–N3B | 120.1 (6) | S1B–O2B | 1.463 (4) | O11–S1B–O3B | 112.4 (3) | | | | |
| | C1B–N3B | 1.314 (6) | N2B–C1B–N3B | 120.4 (6) | S1B–O3B | 1.448 (4) | O12–S1B–O3B | 113.2 (3) | | | | |
| 4 | C1–N1 | 1.312 (5) | N1–C1–N2 | 120.2 (2) | S1–O11 | 1.452 (3) | O11–S1–O12 | 113.0 (1) | N11–O24 | 1.194 (6) | O24–N11–O25 | 124.0 (5) |
| | C1–N2 | 1.318 (4) | N1–C1–N2A | 120.2 (2) | S1–O12 | 1.452 (3) | O11–S1–O12A | 113.0 (1) | N11–O25 | 1.212 (7) | | |
| | C1–N2A | 1.318 (4) | N2–C1–N2A | 119.5 (4) | S1–O12A | 1.452 (3) | O12–S1–O12A | 110.9 (2) | | | | |
| 5 | C1–N1 | 1.325 (6) | N1–C1–N2 | 119.7 (2) | S1–O1 | 1.462 (3) | O1–S1–O2 | 111.7 (1) | | | | |
| | C1–N2 | 1.320 (4) | N1–C1–N2A | 119.7 (2) | S1–O2 | 1.462 (2) | O1–S1–O2A | 111.7 (1) | O–H | *b* | | |
| | C1–N2A | 1.320 (4) | N2–C1–N2A | 120.6 (4) | S1–O2A | 1.462 (2) | O2–S1–O2A | 112.4 (2) | | | | |
| 6 | C1–N1 | 1.323 (3) | N1–C1–N2 | 119.6 (3) | S1–O11 | 1.450 (2) | O11–S1–O12 | 113.8 (1) | C17=O24 | 1.212 (3) | O24=C17–O25 | 122.5 (2) |
| | C1–N2 | 1.322 (3) | N1–C1–N3 | 119.9 (2) | S1–O12 | 1.445 (2) | O11–S1–O13 | 111.2 (1) | C17–O25(H25) | 1.311 (3) | C17–O25–H25 | 111 (2) |
| | C1–N3 | 1.323 (4) | N2–C1–N3 | 120.4 (2) | S1–O13 | 1.465 (2) | O12–S1–O13 | 112.9 (1) | O25–H25 | 0.89 (4) | | |

[a] Note that these H were placed at idealized positions, $d_{N-H}$ = 0.95 Å. [b] The hydroxyl proton was not located in the structure determination.

**Hydrogen Bonding.** Hydrogen bonding strongly directs crystal packing in the guanidinium sulfonate salts. The definition of an X–H···Y hydrogen bond generally relies on intermolecular distance and directionality. An intermolecular distance of less than the sum of the van der Waals radii of the heavy atoms ($d_{X\cdots Y} < d_{vDW(X)} + d_{vDW(Y)}$), assuming a nearly linear X–H···Y angle ($\theta_{X-H\cdots Y} = 180°$), is generally considered as an indication of a hydrogen bond. Using accepted van der Waals radii,[23] the cutoff distance for an N–H···O hydrogen bond is $d_{N\cdots O} = 3.07$ Å, and for an O–H···O hydrogen bond is $d_{O\cdots O} = 3.04$ Å. All hydrogen bonds between guanidinium and sulfonate ions in **1–4** and intraribbon hydrogen bonds between guanidinium and sulfonate ions in **5** and **6** (see following discussion) fall within this distance criterion. The hydrogen bonds range in $d_{N\cdots O}$ length from 2.84 to 3.02 Å (average 2.916 ± 0.112 Å) but deviate from linearity with $\theta_{N-H\cdots O}$ angles ranging from 145.2 to 179.2° (average 165.0 ± 8.2°). Note that, except for **4**, guanidinium hydrogens were placed at idealized positions in the structure determinations, resulting in some uncertainty in the $\theta_{N-H\cdots O}$ angles. The $\theta_{N-H\cdots O}$ angles of **4** were determined using isotropically refined guanidinium hydrogen atom positions. In a previous study of hydrogen bonding in guanidyl carboxylates, distances $d_{N\cdots O} < 3.3$ Å and angles $\theta_{N-H\cdots O} < 33°$ (i.e., greater than 147°) were claimed to meet the criteria for hydrogen bonding.[24] If these distance criteria are applied to the guanidinium sulfonates, the intermolecular interactions in **5**, which were observed to have $d_{N\cdots O} = 3.20$ Å, can be considered hydrogen bonds. Hydrogen bonding and other short intermolecular contacts, which might not be generally classified as hydrogen bonds, between the X substituent and guanidinium or sulfonate acceptor sites are evident in several salts.

The structural features common to guanidinium sulfonates **1–6** are hydrogen-bonded *dimer* interactions **I** [Chart 2, eight-membered *R*ing, graph set[25] motif $R_2^2$ 8)] formed via two amino protons on two nitrogen atoms of a single guanidinium ion and two lone electron pairs on two oxygen atoms of a single sulfonate ion. These dimers will link along one direction to form hydrogen-bonded *ribbons* **II** which, in the absence of perturbing influences from the substituents on the R groups, will further link into *sheets* **III** through $R_2^2(8)$ dimer and $R_6^3(12)$ ring interactions. The guanidinium nitrogens each carry partial positive charges and the sulfonate oxygens each carry partial negative charges; thus, guanidinium···sulfonate hydrogen bonding is also favored by Coulombic forces. Table 3 lists guanidinium sulfonate hydrogen-bond geometries and symmetry relations between ions, describing the structural aspects and symmetries as hydrogen bonding between two dimers (A and B) linked into ribbons **II** (*intra*ribbon), and hydrogen bonding which links these ribbons into sheets **III** through dimer C interactions (*inter*ribbon). For ease of analysis, ribbon orientations

**Chart 2**

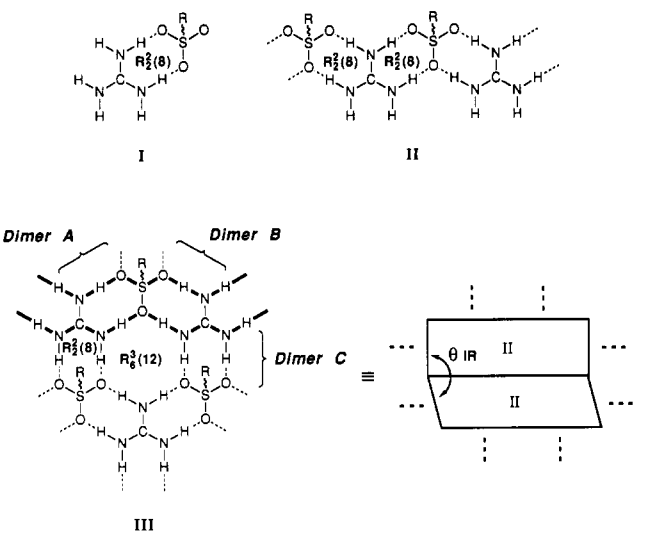


are taken to be either the most planar ribbons (as determined by coplanarity of the guanidinium ion with the sulfonate oxygen plane), or those parallel to specific unit cell directions. Ribbon assignments are discussed later in this section. Note that for each ORTEP representation in Figure 1, the ribbon direction is oriented horizontally approximately in the plane of the paper. The environment of at least one guanidinium ion is depicted in Figure 2 for salts **1**, **4**, **5**, and **6** with schematic representations of the hydrogen bonding (graph set motifs are given **1**, **4**, and **5**; note that the hydrogen-bonded ribbons are oriented nearly horizontally). Hydrogen-bonding and other short intermolecular contact geometries involving the X substituents are given in Table 4.

Hydrogen-bonded sheets **III** are observed in cases where the para-substituent X is a poor hydrogen bonding functionality (salts **1–4**, X = $-CH_3$, $-NH_2$, $-OCH_3$, $-NO_2$) which does not interfere with this guanidinium-sulfonate hydrogen-bonded network. In cases where the para-substituent X is a good hydrogen-bonding functionality, the guanidinium sulfonate hydrogen-bonded network may be disrupted by hydrogen-bonding competition of X for either guanidinium donors and/or sulfonate acceptor sites. In **1–3** only a slight puckering of the hydrogen-bonded sheets occurs, while in **4** the sheets are significantly puckered. A highly puckered network that resembles **III** is observed in **5** (X = –OH); however, the guanidinium–sulfonate interribbon connectivity differs. The sheet motif is fully disrupted in **6** (X = $-CO_2H$). The motifs in **4–6** suggest that increasing hydrogen-bonding ability of X results in increasing competition for the hydrogen bonding sites of the guanidinium–sulfonate network and, consequently, increasing perturbation of the hydrogen-bonded sheet **III**. The degree of puckering can be described by the interribbon dihedral angle, $\theta_{IR}$ (Table 3), which subtends the planes of adjacent ribbons (see equivalent drawing of **III**). This value describes the planarity of the hydrogen-bonded sheets, an ideally planar sheet having $\theta_{IR} = 180°$.

Guanidinium tosylate **1** (X = $-CH_3$) crystallizes in space group $P2_1/c$. Its molecular packing comprises hydrogen-bonded ribbons **II** along the *b*-axis, forming sheet motifs **III** parallel to the *ab* plane (Figure 2). Guanidinium sulfanilate **2** (X = $-NH_2$) and guanidinium *p*-anisolesulfonate **3** (X = $-OCH_3$) are isostructural with **1**, with the

(23) Bondi, A. *J. Phys. Chem.* **1964**, *68*, 441.
(24) Salunke, D. M.; Vijayan, M. *Int. J. Peptide Protein Res.* **1981**, *18*, 348.
(25) Graph set analysis is a method of categorizing hydrogen-bond motifs based on graph theory. A graph set is assigned using the pattern designator (*G*), its degree (*r*), and the number of donors (*d*) and acceptors (*a*), as shown: $G_d^a(r)$. *G* is a descriptor referring to the pattern of hydrogen bonding and has four different assignments: S (self), C (chain), R (ring), and D (dimer or discrete). The degree *r* refers to the number of atoms contained in the ring for R motifs or to the repeat length of the chain for C motifs. Etter, M. C.; MacDonald, J. C.; Bernstein, J. *Acta Crystallogr.* **1990**, *B46*, 256.

**Table 3. Guanidinium-Sulfonate Hydrogen-Bond Geometries for 1–6[a]**

| | intraribbon (dimer A + dimer B) | | | | | | interribbon (dimer C) | | | |
|---|---|---|---|---|---|---|---|---|---|---|
| | dimer A | | | dimer B | | | dimer C | | | |
| compound | symmetry of dimer A ions | $d_{N\cdots O}$ $d_{N\cdots O}$ (Å) | $\theta_{N-H\cdots O}$ $\theta_{N-H\cdots O}$ (deg) | symmetry relating dimer A and dimer B ions | $d_{N\cdots O}$ $d_{N\cdots O}$ (Å) | $\theta_{N-H\cdots O}$ $\theta_{N-H\cdots O}$ (deg) | symmetry of dimer C | $d_{N\cdots O}$ $d_{N\cdots O}$ (Å) | $\theta_{N-H\cdots O}$ $\theta_{N-H\cdots O}$ (deg) | interribbon dihedral angle $\theta_{IR}$ (deg) |
| 1 | asymmetric unit | | | transl along $y$ | | | asymmetric unit | | | |
| | N3–H5···O2 | 2.952 (4) | 162.44 | N3–H6···O1 | 2.951 (4) | 160.47 | N1–H2···O12 | 2.945 (4) | 149.01 | 151 |
| | N2–H4···O3 | 2.921 (4) | 174.24 | N1–H1···O3 | 2.898 (4) | 167.41 | N2–H3···O13 | 2.909 (4) | 155.73 | |
| | transl along $y$ | | | asymmetric unit | | | transl along $x$ | | | |
| | N11–H21···O12 | 2.894 (4) | 171.29 | N11–H22···O13 | 2.891 (4) | 179.15 | N13–H25···O1 | 2.930 (4) | 168.15 | |
| | N13–H26···O11 | 2.956 (4) | 158.69 | N12–H23···O11 | 3.008 (4) | 162.99 | N12–H24···O2 | 2.963 (4) | 166.47 | |
| 2 | asymmetric unit | | | transl along $y$ | | | asymmetric unit | | | |
| | N3–H5···O2 | 2.841 (6) | 173.63 | N3–H6···O1 | 2.843 (6) | 164.94 | N1–H2···O12 | 2.855 (6) | 164.75 | 147 |
| | N2–H4···O3 | 3.086 (7) | 155.97 | N1–H1···O3 | 2.996 (7) | 150.44 | N2–H3···O13 | 2.955 (6) | 157.05 | |
| | asymmetric unit | | | transl along $y$ | | | transl along $x$ | | | |
| | N11–H22···O13 | 2.972 (6) | 161.25 | N11–H21···O12 | 2.948 (6) | 163.81 | N12–H24···O2 | 2.918 (6) | 156.95 | |
| | N12–H23···O11 | 2.893 (6) | 176.30 | N13–H26···O11 | 2.920 (6) | 163.96 | N13–H25···O1 | 2.940 (6) | 146.97 | |
| 3 | asymmetric unit | | | transl along $y$ | | | asymmetric unit | | | |
| | N3A–H19···O1B | 2.850 (7) | 170.25 | N3A–H20···O2B | 2.862 (7) | 171.42 | N1A–H16···O1A | 2.914 (6) | 161.00 | 164 |
| | N2A–H17···O3B | 2.925 (7) | 161.40 | N1A–H15···O3B | 2.964 (7) | 159.69 | N2A–H18···O2A | 2.899 (7) | 163.89 | |
| | transl along $x$, $y$ | | | transl along $x$ | | | asymmetric unit | | | |
| | N3B–H26···O3A | 2.940 (7) | 156.59 | N3B–H25···O2A | 2.945 (7) | 160.60 | N2B–H23···O1B | 2.900 (6) | 145.19 | |
| | N1B–H22···O1A | 2.902 (7) | 167.18 | N2B–H24···O3A | 2.904 (7) | 167.32 | N1B–H21···O2B | 2.894 (6) | 149.71 | |
| 4 | asymmetric unit | | | $m \perp a$ | | | $2_1 \parallel c$ | | | |
| | N1–H1···O12 | 2.900 (4) | 177.48 | N1–H1A···O12A | 2.900 (4) | 177.48 | N2–H4···O12A | 3.018 (4) | 169.21 | 72 |
| | N2–H3···O11 | 3.005 (5) | 174.26 | N2A–H3A···O11 | 3.005 (5) | 174.26 | N2A–H4A···O12 | 3.018 (4) | 169.21 | |
| 5 | asymmetric unit | | | $m \perp a$ | | | $c \perp b$[b] | | | |
| | N1–H1···O2 | 2.955 (3) | 168.81 | N1–H1A···O2A | 2.955 (3) | 168.81 | N2–H3···O2A | 3.197 (4) | 133.61 | 51 |
| | N2–H2···O1 | 2.938 (4) | 174.49 | N2A–H2A···O1 | 2.938 40 | 174.49 | N2A–H3A···O2 | 3.197 (4) | 133.61 | |
| 6 | asymmetric unit | | | transl along $x$ | | | | | | |
| | N1–H2···O13 | 2.901 (3) | 170.51 | N1–H1···O12 | 2.932 (3) | 168.39 | | | | |
| | N2–H3···O11 | 2.972 (3) | 168.57 | N3–H6···O11 | 2.896 (3) | 166.03 | | | | |

[a] Note that all guanidinium hydrogens (except in 4) were placed at idealized positions, resulting in uncertainty in the $\theta_{N-H\cdots O}$ angles. [b] Not a cyclic dimer interaction—one ion interacts with two ions of opposite charge.

same hydrogen-bonding motif **III**. The $c$-lattice constants vary slightly between the isostructural salts because of the different sizes of the para substituents, but the $a$ and $b$ lattice parameters, corresponding to the planes of hydrogen bonding, remain fairly constant. The interribbon dihedral angles $\theta_{IR}$ in **1**, **2**, and **3** are 151, 147, and 164°, respectively, indicating puckering similar to that reported for guanidinium benzenesulfonate[14] ($\theta_{IR}$ = 150°).

The structures of guanidinium *p*-nitrobenzenesulfonate **4** (X = $-NO_2$) and guanidinium *p*-hydroxybenzenesulfonate **5** (X = –OH) are similar, although they differ with respect to their centering operations (space groups *Ama*2 and *Ima*2, respectively) and details of the hydrogen-bonded sheet motifs (Figure 2). Both contain hydrogen-bonded ribbons **II** generated by mirror-symmetry-related ion pairs along the $a$ axes. In these salts, the asymmetric units contain only half of a guanidinium and half of a sulfonate ion, and mirror symmetry ($m \perp a$) is imposed on the ions, which generates the hydrogen-bonded ribbons. In **4**, $2_1$ screw-related ribbons are linked to form highly puckered hydrogen-bonded sheets **III** ($\theta_{IR}$ = 72°), whose mean plane of hydrogen bonding is parallel to the $ac$ plane. The ribbons contained in the sheet are connected by $R_2^2(8)$ dimer and $R_6^3(12)$ ring interactions. Hydrogen bonding by the nitro groups in **4** is not evident although there is a weak bifurcated interaction (graph set motif $R_2^1(4)$), which could possibly be considered a very weak, hydrogen bond,[24] between one nitro oxygen of a 2-fold-related sulfonate and two guanidinium protons residing on the same nitrogen atom ($d_{N\cdots O}$ = 3.19 Å, $\theta_{N-H\cdots O}$ = 102°). The $\theta_{N-H\cdots O}$ deviates from linearity due to the bifurcated nature of the interaction. The hydrogen-bonded ribbons in **5** link through weak intermolecular guanidinium–sulfonate interactions (3.20 Å) between the two remaining donors of a *single* guanidinium cation and acceptor sites of *two* sulfonate anions with $R_4^2(10)$ and $R_4^3(10)$ graph set motifs, differing from the motif **III**, in which the ribbons link by hydrogen bonding between *one* guanidinium ion and *one* sulfonate ion in $R_2^2(8)$ and $R_6^3(12)$ graph set motifs. The severe distortion of the hydrogen-bonded network is revealed by the extremely low interribbon dihedral angle, $\theta_{IR}$ = 51°. The two guanidinium protons not involved in the ribbon participate in a bifurcated interaction with the phenolic oxygen of body-centered/*n*-glide-related sulfonate oxygens in a $R_2^1(6)$ motif ($d_{N\cdots O}$ = 3.19 Å, $\theta_{N-H\cdots O}$ = 139.7°). The hydroxyl proton was not located in the structure determination but, on the basis of the position of the hydroxyl oxygen, appears to participate in very weak intermolecular interactions with $z$-translation- (bifurcated) and 2-fold-related sulfonates ($d_{O\cdots O}$ = 3.36 and 3.32 Å, respectively, not shown in Figure 2). The observed molecular arrangement provides for a maximum number of weak intermolecular interactions.

In guanidinium *p*-carboxybenzenesulfonic acid **6** (X = $-CO_2H$), hydrogen-bonded ribbons **II** are observed parallel to the $a$-axis but are not interlinked through guanidinium–sulfonate interactions due to competitive hydrogen bonding of the guanidinium sulfonate sheet motif with the X substituent. The $a$ unit-cell length of 7.19 Å (ribbon direction) in **6** is identical to that in **5**, slightly shorter than the lengths of the unit-cell axes corresponding to the ribbon directions in **1**–**4** (average 7.44 Å). Hydrogen bonding also occurs between the para-substituted carboxyl group and the two remaining guanidinium donors and one of the remaining sulfonate acceptor sites (Figure 2). Each

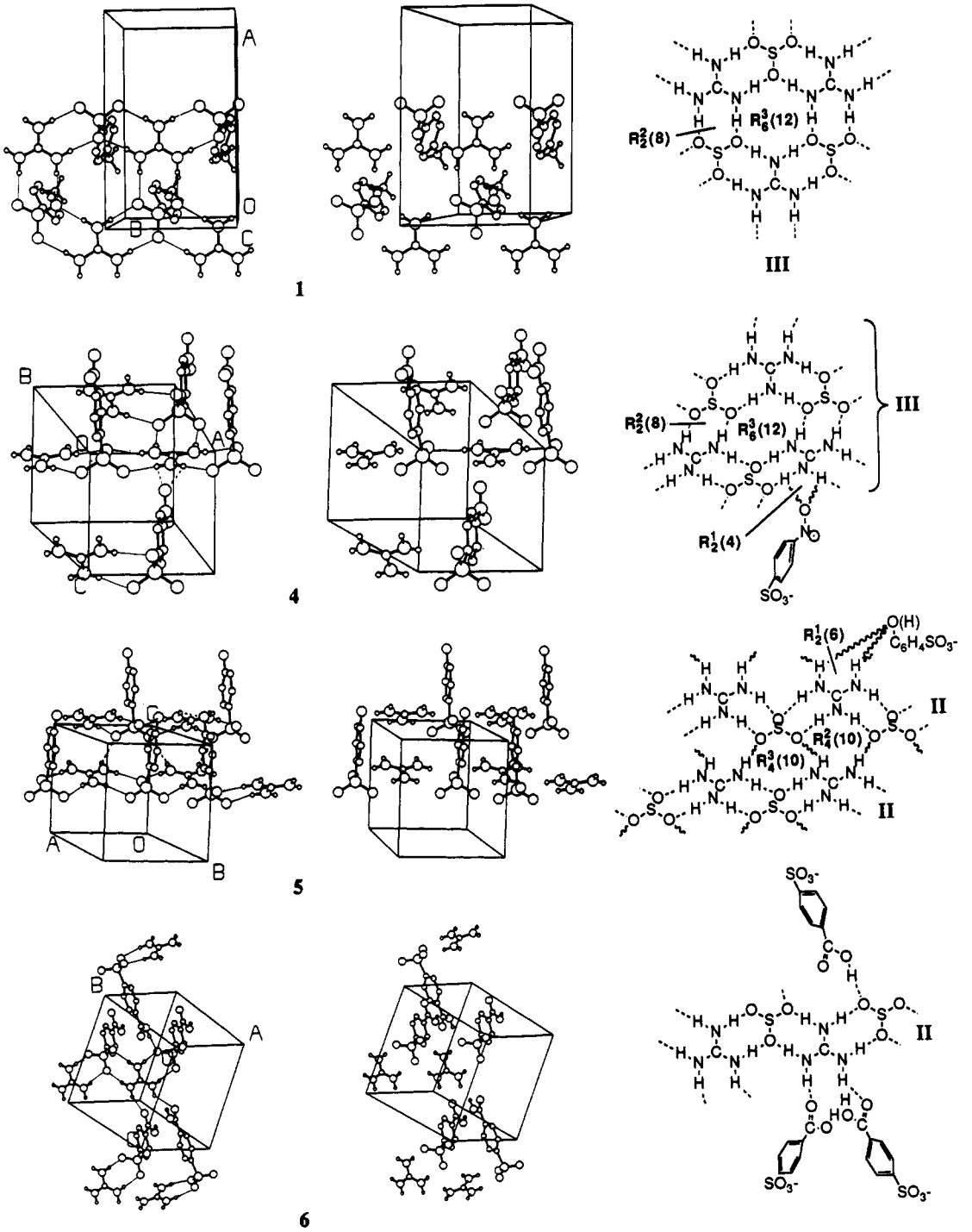


**Figure 2.** Stereoviews (left) showing the hydrogen-bonding environments around guanidinium in salts **1**, **4**, **5**, and **6** and corresponding schematic representations (right) of the hydrogen-bonding motifs. Salts **2** and **3** are isostructural with **1**, and views of these compounds are not shown. In the left-hand stereoviews, hydrogen bonds are indicated by thin lines and short intermolecular contacts by dotted lines. In the corresponding schematic representations on the right, hydrogen bonds are indicated by dashed lines and short intermolecular contacts by wavy lines. Roman numerals in the schematics refer to guanidinium sulfonate hydrogen-bonded ribbons (**II**) and sheets (**III**). The ribbons run approximately left-to-right across the page in both the stereoviews and the schematics. Graph set notations for ring motifs are also indicated in the schematics (see text, ref 25). Graph set assignments for compound **6** are not shown in the schematic (see text, ref 26). Aromatic ring hydrogens have been omitted for clarity.

of the remaining guanidinium donors form hydrogen bonds to carboxyl carbonyl acceptor sites on different sulfonates, one *z*-translationally-related (graph set motif $C_2^2(13)$,[26] $d_{N\cdots O}$ = 2.96 Å) and one $a \perp b$ glide-related (graph set motif $C_2^2(11)$,[26] $d_{N\cdots O}$ = 3.08 Å). One of the two remaining sulfonate acceptor sites forms hydrogen bonds to the carboxyl proton of a $a \perp b$-glide-related sulfonate (graph set motif C(9),[26] $d_{O\cdots O}$ = 2.62 Å); the other acceptor site is not used in hydrogen bonding.

**Layering Motifs.** The guanidinium sulfonates can be classified according to two types of layering motifs,[14] namely bilayer and single layer structures (Scheme 1). In each case, the sulfonate R groups of a given hydrogen-bonded ribbon **II** are all oriented to the same side of the ribbon, but the two layering motifs differ with respect to the relative orientation of sulfonate R groups on *adjacent* ribbons which assemble into sheets **III**. Bilayer packing occurs when all R groups of adjacent ribbons are oriented

**Table 4. Non-Guanidinium–Sulfonate Hydrogen-Bond and Short Contact Geometries for 4–6**

| compound | nature of contact X–H···Y | symmetry relation | | $d_{X\cdots Y}$ (Å) | $\theta_{X-H-Y}$ (deg) |
|---|---|---|---|---|---|
| 4 | $NH_2$···O–N(–O) | $2 \parallel c$, | N1–H1···O25 | 3.192 (6) | 102.00 |
| | bifurcated | $m \perp a$ | N1–H1A···O25 | 3.192 (6) | 102.00 |
| 5 | C–$(NH)_2$···O(H) | *I*-centering, | N2–H3···O4 | 3.188 (4) | 139.70 |
| | bifurcated | $n \perp a$ | N2A–H3A···O4 | 3.188 (4) | 139.70 |
| | S–O···(H)O | $2 \parallel c$ | O2···(H)–O4 | 3.317 (3) | *a* |
| | S–O···(H)O | transl along *z*, | O2···(H)–O4 | 3.358 (4) | *a* |
| | bifurcated | $m \perp a$ | O2A···(H)–O4 | 3.358 (4) | |
| 6 | S–O···HOOC | $2_1 \parallel b$ | O13···H25–O25 | 2.624 (3) | 168.10 |
| | N–H···O=C | transl along *z* | N3–H5···O24 | 2.956 (3) | 154.02 |
| | N–H···O=C | $a \perp b$ | N2–H4···O24 | 3.076 (3) | 137.16 |
| | N–H···O=C | transl along *z* | N2–H4···O24 | 3.297(3) | 124.78 |

[a] The hydroxyl proton was not located in the structure determination.

**Scheme 1**

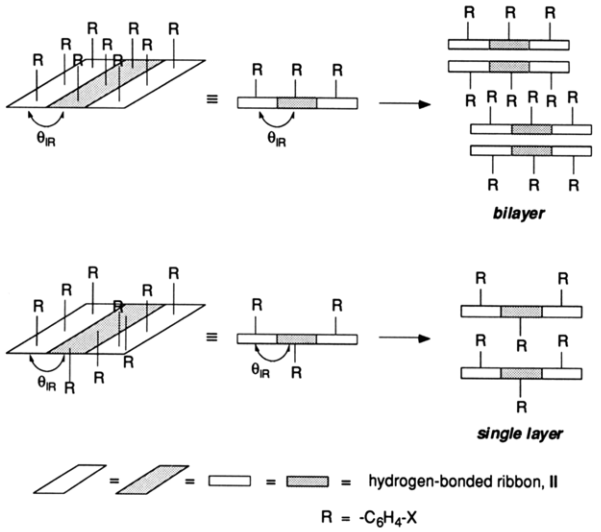


to the *same* side of the hydrogen-bonded plane, and single-layer packing occurs when the orientation of the R groups of adjacent ribbons *alternates* across the hydrogen-bonded plane in a direction normal to the ribbons.

X-ray crystal-packing diagrams illustrating the types of layer packings for **1–6** are presented in Figures 3 and 4. Note that hydrogen-bonded ribbon directions are oriented normal to the page in both the stereoviews and schematic representations. Salts **1**, **2**, and **3** each crystallize with the typical hydrogen-bond sheet motif **III** arranged in bilayer structures. In these structures edge-to-face interactions of aryl rings occur between neighboring hydrogen-bonded layers. Salts **4** and **5** contain highly puckered hydrogen-bonded sheets arranged in single-layer type structures, with hydrogen-bonded ribbons connected by the typical (one guanidinium:one sulfonate) dimer **I** interaction in **4**, but by (one guanidinium:two sulfonate) interactions in **5** (Figure 2). Although the sheet motifs of **4** and **5** differ slightly, they are similar topologically in that the sulfonate R groups alternate orientation in adjacent ribbons. Both **4** and **5** are noncentrosymmetric, with all nitro or hydroxyl groups oriented along the polar *c* axes. Face-to-face aryl $\pi$-stacking interactions occur between hydrogen-bonded layers in **4** and **5**. Compound **6** contains only hydrogen-bonded ribbons **II**, which do not link into sheets, and thus does not have either type of layer structure shown in Scheme 2. The packing patterns of each salt **1–6** result in partitioning into hydrophobic regions containing the aromatic sulfonate R groups and polar regions containing the guanidinium-sulfonate hydrogen bonding networks.

## Discussion

The hydrogen-bond motifs and preferred solid-state packing patterns of guanidinium with organic (R) sulfonates in which hydrogen-bonding functionality on the R groups is absent have been reported previously.[14] These salts were found to crystallize into two-dimensional hydrogen-bonded sheets (**III**), in which all six guanidinium protons were used in hydrogen bonding to all six sulfonate oxygen electron lone pairs. The packing of these salts in the third dimension was determined by the size of the sulfonate R groups, with packing into either bilayer structures for smaller R groups (e.g., methyl or phenyl) or into single layer structures for bulky R groups (e.g., 1-naphthyl or (1*S*)-(+)-10-camphoryl). All of these structures were centrosymmetric, with the exception of the chiral (1*S*)-(+)-10-camphorsulfonate salt.

The compounds described in this report reveal the influence of R-group substituents with hydrogen-bonding capability on the hydrogen-bonded sheet motif. Whereas simple alkane- and arenesulfonates and the arenesulfonates of compounds **1–3** influence the sheet structure solely by steric effects, compounds **4–6** exhibit sheet motifs that are perturbed considerably by the R-group substituent. In the latter compounds the interribbon linkage that generally directs the formation of planar hydrogen-bonded sheets with the motif **III** arranged in bilayer structures (large $\theta_{IR}$) is disrupted by competitive hydrogen bonding of the para-substituent X with either guanidinium or sulfonate hydrogen-bonding sites. This perturbation, as surmised from the structural details and the degree of sheet puckering, increases with increasing hydrogen-bonding ability of para-substituent X.

**Competitive Hydrogen Bonding: Effect of X on Crystal Packing.** Compounds **1–6** possess guanidinium sulfonate hydrogen-bonded dimers **I** linked into ribbons **II**. This ribbon motif is present in all guanidinium sulfonate structures we have studied thus far. The dimer linkage **I** is analogous to that found in biologically relevant systems such as guanidyl carboxylates and phosphates,[24,27] which often contain arrangements of two nearly parallel N–H···O hydrogen bonds as in **II**. Guanidyl-sulfonate hydrogen-bonded dimers[28] and ribbons[29] are also found in many other compounds. Our results clearly indicate

(26) Graph set assignments for salt **6** are made by considering the chains (C) starting at the symmetry-related hydrogen-bonding site and running through the asymmetric unit by the shortest path to determine the repeat length *r*. Thus, the graph set for the hydrogen bond between guanidinium and the carbonyl oxygen of a *z*-translationally-related sulfonate is $C_2^2(13)$ (i.e., ···H5–N3–C1–N1–H2···O–S1–C–C–C–C–C17–O24···); between guanidinium and the carbonyl oxygen of an $a \perp b$ glide-related sulfonate is $C_2^2(11)$ (i.e., ···H4–N2–H3···O–S1–C–C–C–C–C17–O24···); and between sulfonate oxygen and the carboxylic acid proton of a $2_1$ screw-related sulfonate is C(9) (i.e., ···O13–S1–C–C–C–C–C17–O25–H25···).

(27) (a) Yokomori, Y.; Hodgson, D. J. *Int. J. Peptide Protein Res.* **1988**, *31*, 289. (b) Adams, J. M.; Small, R. H. W. *Acta Crystallogr.* **1976**, *B32*, 832. (c) Adams, J. M.; Ramdas, V. *Acta Crystallogr.* **1976**, *B32*, 3224.

(28) (a) Doubell, P. C. J.; Oliver, D. W.; Van Rooyen, P. H. *Acta Crystallogr.* **1991**, *C47*, 353. (b) Griffin, R. J.; Meek, M. A.; Schwalbe, C. H.; Stevens, M. F. G. *J. Med. Chem.* **1989**, *32*, 2468. (c) Sutton, P. A.; Cody, V. *J. Cryst. Spectros. Res.* **1988**, *18*, 755. (d) Cody, V. *Acta Crystallogr.* **1984**, *C40*, 1000. (e) Cody, V.; Zakrzewski, S. F. *J. Med. Chem.* **1982**, *25*, 427. (f) Destro, R.; Maghini, A.; Merati, F. *Acta Crystallogr.* **1987**, *C43*, 949. (g) Kim, Y. B.; Wakahara, A.; Fujiwara, T.; Tomita, K.-I. *Bull. Chem. Soc. Jpn.* **1973**, *46*, 2194. (h) Pitman, I. H.; Shefter, E.; Ziser, M. *J. Am. Chem. Soc.* **1970**, *92*, 3413.

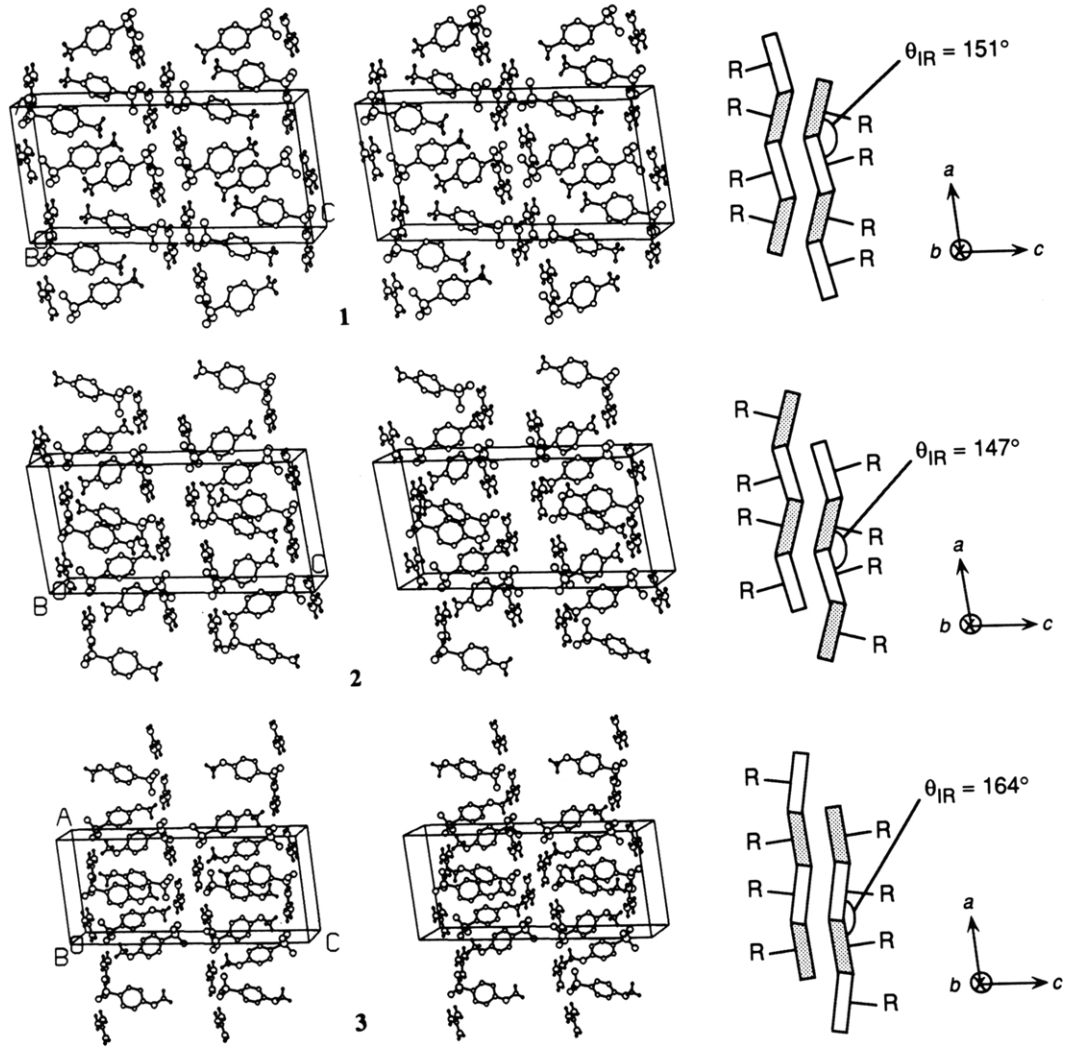


**Figure 3.** Stereoviews (left) illustrating the bilayer motifs of **1–3**, in which para-substituents X do not perturb the hydrogen-bonded sheet motif **III**, and schematic representations (right) of the layered structures (see Scheme 1 for interpretation). Note that the guanidinium–sulfonate hydrogen-bonded ribbons project normal to the plane of the paper in both the stereoviews and schematics. Aromatic ring hydrogens have been omitted for clarity.

that this ubiquitous ribbon motif can be used confidently as a design element in derivatives of these materials.

However, the design of materials based on guanidinium sulfonates hinges on the subsequent assembly of these ribbons into two-dimensional sheets and further layering of the sheets into the three-dimensional solid. The two-dimensional hydrogen-bond motif in guanidinium sulfonates probably results from a combination of stabilizing factors: the large number of hydrogen bonds, matched number of donors and acceptors, 3-fold topologies for both the guanidinium and $RSO_3^-$ ions, and Coulombic interactions between oppositely charged ions. General hydrogen-bonding rules formulated by our group[10] predict that the best hydrogen-bond donor and the best hydrogen-bond acceptor will form hydrogen bonds with each other. Subsequent hydrogen bonding pairs comprise the second-best donor and second-best acceptor, and so on. If X is a better hydrogen-bond donor than guanidinium or a better hydrogen-bond acceptor than sulfonate, we would expect the sheet motif to be perturbed as a result of competitive hydrogen bonding by X. However, it can be difficult to evaluate the hydrogen-bonding abilities of molecules with multiple hydrogen bonding sites, as the hydrogen-bonding ability of each site will be influenced by cooperativity effects involving the other sites.

Our previous results and the crystal structures of **1–3** clearly indicate that nearly planar, two-dimensional hydrogen-bonded sheets of motif **III** are preserved in the absence of R group hydrogen-bonding functionality, for R groups of width <4.75 Å.[14] The slight sheet puckering observed in the bilayer structures can be attributed to a combination of steric effects and favorable van der Waals R–R interactions between hydrogen-bonded layers. Our results reveal that the para-amino group in **2** is not a good enough hydrogen-bond donor to compete with guanidinium···sulfonate hydrogen bonding. The methoxyl oxygen in **3**, which rarely acts as a hydrogen-bond acceptor, also does not affect the sheet motif. When the weakly accepting group $NO_2$ is the substituent, the guanidinium-sulfonate hydrogen-bond sheet retains its general characteristics, forming the motif **III** with the $R_2^2(8)$ and $R_6^3(12)$ graph set motifs. However, the guanidinium–sulfonate hydrogen-bonded ribbons **II** along the *a*-direction are connected to one another in a nearly *orthogonal* manner, forming a highly puckered single-layer type structure. This finding was somewhat unexpected because

(29) (a) McCourt, M.; Cody, V. *J. Am. Chem. Soc.* **1991**, *113*, 6634. (b) Matsumoto, O.; Taga, T.; Machida, K. *Acta Crystallogr.* **1989**, *C45*, 913. (c) Nakamura, H.; Iitaka, Y. *Acta Crystallogr.* **1978**, *B34*, 3384. (d) Bombieri, G.; Demartin, F.; Grabhiroli, D.; Di Bella, M. *J. Cryst. Spectrosc. Res.* **1990**, *20*, 403.

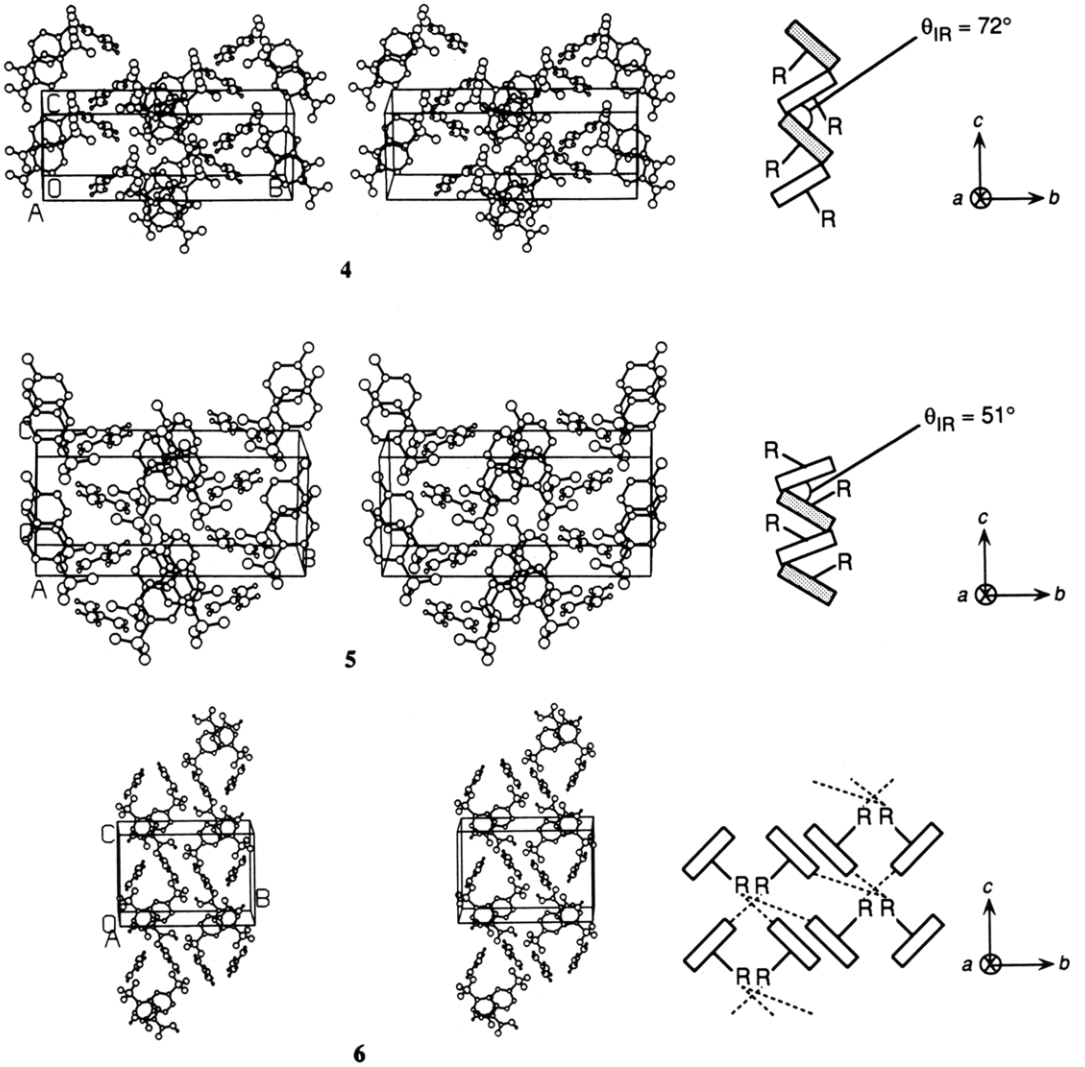


**Figure 4.** Stereoviews (left) illustrating the single layer motifs of **4** and **5** and an analogous view of **6** and schematic representations (right) of the layered structures (see Scheme 1 for interpretation). Note that the guanidinium sulfonate hydrogen-bonded ribbons project normal to the plane of the paper in both the stereoviews and schematics. Dashed lines in the schematic for **6** indicate hydrogen bonding between the carboxyl group and a neighboring ribbon. Aromatic ring hydrogens have been omitted for clarity.

the nitro group in **4** is generally considered to be a relatively poor hydrogen-bond acceptor and would not be expected to interfere with the hydrogen-bonded bilayer structure (a structure similar to **1** was predicted). Nevertheless, the sheet is perturbed by a weak bifurcated intermolecular interaction between one nitro oxygen and two protons attached to the same guanidinium nitrogen ($d_{N\cdots O}$ = 3.19 Å). Face-to-face aryl–aryl $\pi$-stacking interactions are observed in **4**, but edge-to-face interactions are present in **1–3**.

The influence of stronger hydrogen bonding on the sheet motif is clearly evident in **5**, in which the hydroxyl group significantly perturbs the guanidinium–sulfonate interactions, that otherwise would lead to motif **III**. The ribbons **II** are linked into a different sheet motif through what might be considered extremely weak guanidinium···sulfonate hydrogen bonds ($d_{N\cdots O}$ = 3.20 Å) with $R_4^2(10)$ and $R_4^3(10)$ graph set motifs. Each guanidinium cation is involved in intermolecular interactions with four sulfonate anions, rather than the usual three. Intermolecular interactions also occur between the phenol group and the guanidinium ion ($d_{N\cdots O}$ = 3.19 Å). The phenol group often acts as both hydrogen-bond donor and acceptor in solid-state structures and is considered to be a better donor than an amino proton, consistent with *direct* interaction of the phenol group with the hydrogen-bonded ribbons. The weak intermolecular contacts between the guanidinium ion and the phenolic oxygen and between oxygens of two sulfonates and the phenolic proton suggest that the hydroxyl group is located so as to maximize a number of weak interactions.

The guanidinium sulfonate hydrogen-bonded network **III** is *completely* disrupted in **6**, where X = $-CO_2H$. The carboxyl group is an excellent hydrogen-bonding group, as is evident from the familiar carboxylic acid dimer interaction,[30] acting as both hydrogen-bond donor and acceptor in **6**. On the basis of acidity arguments ($pK_{a2}$(*p*-$HO_3SC_6H_4CO_2H$) = 3.72;[31] $pK_a$(guanidinium) = 13.5[32]), the carboxylic acid proton is a better donor than guanidinium, which would favor hydrogen bonding of the strongly donating carboxyl proton to the good sulfonate acceptor. Interaction with the good sulfonate acceptor also explains the absence of carboxyl–carboxyl dimer interactions as the carbonyl oxygen is a relatively poor acceptor.

(30) Leiserowitz, L. *Acta Crystallogr.* **1976**, *B32*, 775.
(31) *Lange's Handbook of Chemistry*; Dean, J. A., Ed.; McGraw-Hill: New York, 1985; Table 5–8, p 5–57.
(32) Charlot, G.; Tremillon, B. *Chemical Reactions in Solvents and Melts*; Pergammon Press: Oxford, 1969; p 80.

**Noncentrosymmetry and SHG Properties of 4 and 5.** In the design of materials for SHG, there are two main requirements: that a material possess a bulk noncentrosymmetric (acentric) structure and that the molecules have a high molecular hyperpolarizability ($\beta$). In this work we have chosen to focus on investigation of solid-state molecular packing modes and how this relates to the design of acentric structures, with the aim of incorporating molecules with high $\beta$ values into the guanidinium–sulfonate networks at a later date. Guanidinium sulfonates are unique because of the symmetries of the guanidinium ion and the $SO_3$ groups. Use of these 3-fold symmetrical groups may be a good choice for the design of acentric materials because of the inherent noncentrosymmetry of the 3-fold axis and the strongly directing influence of hydrogen bonding, which preserves the general sheet motif. In addition, the ionic nature of the guanidinium–sulfonate sheets may serve to screen interactions between molecular dipoles in neighboring layers that otherwise would favor the formation of centrosymmetric phases. Indeed, we found **4** and **5** to crystallize in acentric space groups, although this may be assisted by the absence of strong donor–acceptor substituents which would provide strong dipolar interactions that may provide the driving force for centrosymmetric phases. Qualitative tests for SHG show both materials to have signals 0.5–0.75 × urea. Although these values are not large, this is not unexpected since neither compound has a large molecular hyperpolarizability.

Another consideration in the design of SHG-active materials is optimization of an acentric lattice. Some acentric lattices, such as $P2_12_12_1$, in which molecular dipoles nearly cancel, are only slightly different from centric ones and have poor SHG activity. Materials crystallizing in point groups 1 (triclinic), 2 or *m* (monoclinic), or *mm*2 (orthorhombic) are most suitable for phase matching.[33] Guanidinium *p*-nitro- and *p*-hydroxybenzenesulfontes, **4** and **5**, crystallize in optimum point group *mm*2 (space groups *Ama*2 and *Ima*2, respectively) and exhibit SHG. The optimum angle of alignment of molecular axis with the polar crystallographic axis for phase matching in the case of point group *mm*2 is 54.74°. The SHG signal is maximized when molecular dipoles are oriented in this optimal direction relative to the optic axis of the crystal. In the case of **4**, the molecular dipole axis is 47° from the polar *c*-axis in the crystal. In **5**, the molecular dipole is 29° from the polar *c*-axis. The deviation from the optimal angle of 54.74°, as well as low $\beta$ values, may explain the low SHG activity of these salts.

(33) Zyss, J.; Oudar, J. L. *Phys. Rev. A* **1982**, *26*, 2028.

## Conclusion

The single-crystal X-ray structures of guanidinium para-substituted benzenesulfonates clearly indicate that the degree of distortion of hydrogen-bonded sheets and the preference for bilayer versus single layer structures is dictated by the hydrogen-bonding ability of para-substituent X. The nearly planar, two-dimensional hydrogen-bonded guanidinium-sulfonate sheet motif is increasingly perturbed as the substituent X increases in hydrogen-bonding ability due to competitive hydrogen bonding of X for guanidinium and/or sulfonate hydrogen-bonding sites. The sheet motif with bilayer structure is preserved for those sulfonate salts having poor hydrogen-bonding ability (X = $-CH_3$, $-NH_2$, $-OCH_3$). The sheets pucker severely and the three-dimensional layering motif changes to a single-layer motif when X interacts with the guanidinium–sulfonate network (X = $-NO_2$, $-OH$). The sheet is completely disrupted when X is an excellent hydrogen-bonding group (X = $-CO_2H$). The strong tendency of guanidinium benzenesulfonates to form guanidinium–sulfonate networks coupled with the flexibility of altering hydrogen-bonding substituents represents a viable approach to molecular-level engineering of new materials. For example, short intermolecular contacts between X and guanidinium ion in **4** and **5** result in crystallization into noncentrosymmetric space groups and SHG activity. Hydrogen-bonding and Coulombic interactions in these salts may override and screen dipolar interactions which often bias molecules to pack in centrosymmetric arrangements. We anticipate that use of sulfonates with higher molecular hyperpolarizabilites will lead to materials with improved second-harmonic generation.

**Acknowledgment.** We gratefully acknowledge the crystallographic assistance of Professor Doyle Britton and Elise Sudbeck of the University of Minnesota. This work was supported by the Office of Naval Research (N0014-89-K-1301).

**Supplementary Material Available:** Anisotropic thermal parameters, intra- and intermolecular bond lengths and angles, and ORTEP drawings for six crystal structures (154 pages); tables of observed and calculated structure factors (107 pages). Ordering information is given on any current masthead page.